A&A 561, L1 (2014)
DOI: 10.1051/0004-6361/201323067


Astronomy & Astrophysics

Letter to the Editor

# SOPHIE velocimetry of *Kepler* transit candidates

## X. KOI-142 c: first radial velocity confirmation of a non-transiting exoplanet discovered by transit timing⋆,⋆⋆

S. C. C. Barros[1], R. F. Díaz[1,7], A. Santerne[1,2], G. Bruno[1], M. Deleuil[1], J.-M. Almenara[1], A. S. Bonomo[5], F. Bouchy[1], C. Damiani[1], G. Hébrard[3,4], G. Montagnier[3,4], and C. Moutou[6,1]

[1] Aix Marseille Université, CNRS, LAM (Laboratoire d'Astrophysique de Marseille) UMR 7326, 13388 Marseille, France
e-mail: susana.barros@lam.fr
[2] Centro de Astrofísica, Universidade do Porto, rua das Estrelas, 4150-762 Porto, Portugal
[3] Institut d'Astrophysique de Paris, UMR7095 CNRS, Université Pierre & Marie Curie, 98bis boulevard Arago, 75014 Paris, France
[4] Observatoire de Haute-Provence, Université d'Aix-Marseille & CNRS, 04870 Saint Michel l'Observatoire, France
[5] INAF – Osservatorio Astrofisico di Torino, via Osservatorio 20, 10025 Pino Torinese, Italy
[6] CNRS, Canada-France-Hawaii Telescope Corporation, 65-1238 Mamalahoa Hwy., Kamuela, HI 96743, USA
[7] Observatoire Astronomique de l'Université de Genève, 51 chemin des Maillettes, 1290 Versoix, Switzerland

Received 15 November 2013 / Accepted 25 November 2013

**ABSTRACT**

The exoplanet KOI-142b (Kepler-88b) shows transit timing variations (TTVs) with a semi-amplitude of ∼12 h, which earned it the nickname "king of transit variations". Only the transit of planet b was detected in the *Kepler* data with an orbital period of ∼10.92 days and a radius of ∼0.36 $R_{\rm Jup}$. The TTVs together with the transit duration variations of KOI-142b were analysed recently, finding a unique solution for a companion-perturbing planet. An outer non-transiting companion was predicted, KOI-142c, with a mass of $0.626 \pm 0.03$ $M_{\rm Jup}$ and a period of $22.3397^{+0.0021}_{-0.0018}$ days, which is close to the 2:1 mean-motion resonance with the inner transiting planet. We report an independent confirmation of KOI-142c using radial velocity observations with the SOPHIE spectrograph at the Observatoire de Haute-Provence. We derive an orbital period of $22.10 \pm 0.25$ days and a minimum planetary mass of $0.76^{+0.32}_{0.16}$ $M_{\rm Jup}$, both in good agreement with the predictions by previous transit timing analysis. Therefore, this is the first radial velocity confirmation of a non-transiting planet discovered with TTVs, providing an independent validation of the TTVs technique.

**Key words.** planetary systems – stars: fundamental parameters – techniques: spectroscopic – techniques: radial velocities – stars: individual: KIC5446285 – stars: individual: Kepler-88

## 1. Introduction

Miralda-Escudé (2002), Holman & Murray (2005), and Agol et al. (2005) have proposed transit timing variation (TTVs) as an additional exoplanet discovery tool. These authors showed that the mutual gravitational interaction of planets close to mean-motion resonances can be strong enough to have a measurable effect on otherwise strictly periodic transit times and are sensitive to masses lower than the current radial velocity (RV) sensitivity limit. Despite several ground-based efforts to detect TTVs in hot-Jupiter systems (e.g. Miller-Ricci et al. 2008; Gibson et al. 2009; Barros et al. 2013) it was only possible to confirm them with the space-based *Kepler* transiting survey. The first TTV exoplanet system discovered, Kepler-9 (Holman et al. 2010), is composed of pair of transiting Saturn-mass planets near the 2:1 resonance and an inner earth-sized companion. Since then, dynamic analyses of TTVs in *Kepler* transiting multi-planetary systems have allowed a better characterisation of the system and/or helped confirm the planetary nature of many candidates (e.g. Holman et al. 2010; Lissauer et al. 2011a; Steffen et al. 2012a). However, for cases where only one of the planet transits, it has been shown that, in general, the TTV inversion problem is degenerate (Nesvorný & Morbidelli 2008; Meschiari & Laughlin 2010; Veras et al. 2011; Boué et al. 2012; Ballard et al. 2011). Only for two special cases, KOI-872 and KOI-142, a unique solution for the companion was found (Nesvorný et al. 2012, 2013).

KOI-142b (Kepler-88b) shows strong TTVs with a semi-amplitude of ∼12 h and a period of 630 days (Ford et al. 2011; Steffen et al. 2012b; Mazeh et al. 2013). Transit duration variations (TDVs) with smaller amplitude (5 min) and in phase with the TTVs were also found (Nesvorný et al. 2013). A dynamic analysis of this system led to the prediction of a non-transiting companion, planet c, with a mass of $0.626 \pm 0.03$ $M_{\rm Jup}$, orbital period of $22.3397^{+0.0021}_{-0.0018}$ days, inclination of $86.2 \pm 1.5°$, and eccentricity of $0.05628 \pm 0.0021$ (Nesvorný et al. 2013). Therefore, the second planet is just wide of the 2:1 resonance with the transiting planet. In this configuration, the resonant angles, which measure the displacement of the longitude of the conjunction from the periapsis of each planet, circulate (or librate) with a period of 630 days. The high amplitude TTVs and TDVs reflect the resonant angle libration.

⋆ Based on observations collected with the NASA *Kepler* satellite and with the SOPHIE spectrograph on the 1.93-m telescope at Observatoire de Haute-Provence (CNRS), France.
⋆⋆ Tables 2 and 3 are available in electronic form at http://www.aanda.org

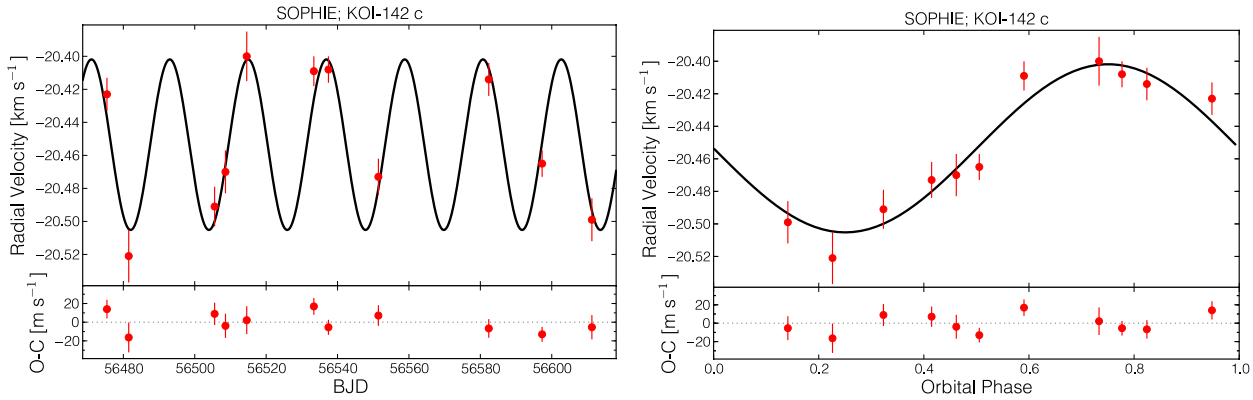


**Fig. 1.** SOPHIE radial velocities as a function of time (*left*) and orbital phase (*right*) and the corresponding residuals. The overplotted black curve is the most probable fit model.

As part of our campaign to validate and characterise *Kepler* transiting exoplanet candidates (e.g. Bouchy et al. 2011; Santerne et al. 2012) we observed KOI-142 with the SOPHIE spectrograph at the Observatoire de Haute-Provence. Although we did not detect the known transiting planet in the system, we detected a clear RV signature of a planet companion with a period of $22.10 \pm 0.25$ days and a minimum mass of $0.76^{+0.32}_{0.16}\ M_{\rm Jup}$, which agrees with the predictions of Nesvorný et al. (2013). In this paper, we present the radial velocity confirmation of KOI-142 c, which is the first RV confirmation of a planet discovered by TTV analysis. We begin by describing the RV observations in Sect. 2. In Sect. 3, we present the host star stellar parameters, and in Sect. 4 we give details on our RV fitting procedure and present the results. We close with a discussion in Sect. 5.

## 2. SOPHIE spectroscopy and velocimetry

We obtained 11 spectroscopic observations of KOI-142 from 1 July 2013 to 14 November 2013 with the SOPHIE spectrograph mounted on the 1.93 m telescope at the Observatoire de Haute-Provence (Perruchot et al. 2008; Bouchy et al. 2009). SOPHIE is a thermally stable high-resolution echelle optical spectrograph fed by a fiber link from the Cassegrain focus of the telescope. The fiber has a diameter of 3″ on sky. The observations were obtained in the high-efficiency (HE) mode, which has a resolution $R \sim 40\,000$ and covers a wavelength range of 390−687 nm.

The radial velocities were derived with the SOPHIE pipeline by computing the weighted cross-correlation function (CCF; Baranne et al. 1996; Pepe et al. 2002) with a G2 mask. The extracted RVs included corrections for charge transfer inefficiency of the SOPHIE CCD (Bouchy et al. 2009) using the procedure described in Santerne et al. (2012). The SOPHIE HE mode exhibits instrumental variations at long time-scales with an amplitude of a few m s$^{-1}$. These were corrected for using observations of a bright and stable star, HD 185144, obtained on the same nights and with the same instrument setup.

Three spectra of KOI-142 that were affected by the Moon-scattered light were corrected for following a procedure similar to the one described by Bonomo et al. (2010).

The average signal-to-noise ratio of each spectra is 23 per pixel at 5800 Å and the average RV uncertainty is 11 m s$^{-1}$. The measurements and the respective uncertainties are given in Table 2. In the same table we also list the exposure time, signal-to-noise ratio per pixel and the bisector span of the cross-correlation function. The fact that the bisector spans of KOI-142 do not vary significantly implies that the stellar CCF is not strongly blended with another star. We describe the RV analysis in the Sect. 4 after deriving the host star stellar parameters.

## 3. Host star

After correcting for RV variations and background contamination, all spectra of KOI-142 were co-added. The signal-to-noise ratio of the resulting spectrum is ∼180 per resolution element at 5800 Å. The atmospheric parameters were derived using the versatile wavelength analysis package (VWA Bruntt et al. 2010a,b) by minimising the correlation between the FeI and FeII abundances and the excitation potential and equivalent width of the spectral lines. The surface gravity ($\log g$) was measured by imposing that the abundances of FeI and FeII are the same, while also checking the consistency with the pressure-sensitive lines Ca I at 6122 Å and 6162 Å. This yielded $T_{\rm eff} = 5460 \pm 70$ K, $\log g = 4.6 \pm 0.2$ dex, [Fe/H] $= 0.25 \pm 0.09$ dex and velocity of microturbulence $v_{\rm micro} = 1.3 \pm 0.1$ km s$^{-1}$, implying a G6 V spectral type. Systematic uncertainties were added in quadrature to the VWA error estimates for $T_{\rm eff}$ and $\log g$ following Bruntt et al. (2010b). Our measurements agree with previously reported values (Nesvorný et al. 2013). The $v \sin i$ was estimated in conjunction with the macroturbulence velocity $v_{\rm macro}$ on a set of isolated spectral lines, yielding $v \sin i = 2 \pm 1$ km s$^{-1}$ and $v_{\rm macro} = 1 \pm 1$ km s$^{-1}$. The good quality of the combined spectrum of KOI-142 allowed us to isolate 321 unbroadened spectral lines, which were used for the analysis. These also permitted us to derive a detailed chemical composition, which is given in Table 3.

## 4. Radial velocity analysis

The radial velocities of KOI-142 show an amplitude of variation of ∼100 m/s (Fig. 1). A generalised Lomb Scargle periodogram (Zechmeister & Kürster 2009) of the RV measurements shows a peak near 22 days, with a false-alarm probability (FAP) below 10% (Fig. 2). This period coincides with the period of the planet discovered by Nesvorný et al. (2013) by transit variation analysis of the KOI-142b planet. The periodogram also shows a lower peak at the first harmonic, with a higher FAP. The Kepler light curve shows a periodicity associated with spot variability at ∼30 days, which is weak in our RV data.

To determine weather the 22-day period corresponds to the planet predicted by Nesvorný et al. (2013), we analysed the

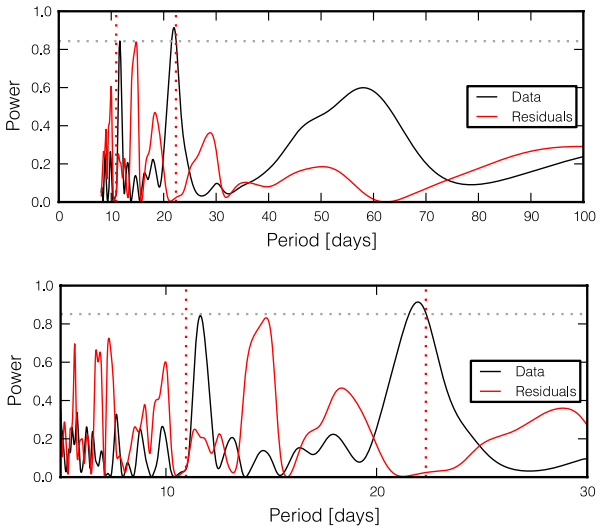


**Fig. 2.** *Top*: generalised Lomb Scargle periodogram of the SOPHIE RV data. A peak is present at around 22 days. The FAP 10% level is shown as a dashed horizontal line. The periods reported by Nesvorný et al. (2013) are marked with vertical dashed lines. The Lomb Scargle periodogram of the residuals is shown in red. *Bottom*: zoom for periods between 5 and 30 days.

SOPHIE RVs of the KOI-142 system using the MCMC algorithm described in detail in Díaz et al. (2013). The RV amplitude expected for the inner planet is 2.58 ± 0.74 m s$^{-1}$ (Nesvorný et al. 2013), which would not be detectable with our current data. Therefore, we decided to use a single Keplerian model at the period of the outer, more massive companion. Note that the signal is not expected to be strictly periodic because of the influence of the inner planet, which changes the orbital parameters of the companion. The change in the orbital parameters of the putative outer planet has been studied in detail by Nesvorný et al. (2013), who showed that the eccentricity remains well constrained for at least 150 years. A numerical integration of the system up to the epoch of the SOPHIE observations was performed using the hybrid symplectic algorithm implemented in the Mercury6 code (Chambers 1999), and taking as initial conditions the values given in Table 2 of Nesvorný et al. (2013). We found that during the time of the SOPHIE observations, the orbital elements of KOI-142b change significantly, while the expected change for the proposed companion at 22 days is much smaller[1] than the precision obtained in these parameters (see Table 1). Therefore, although it is not exactly correct, using a Keplerian curve to model the signal induced by the second companion is justified for the period of the SOPHIE observations.

Uninformative priors were used in all parameters of the model. In this case, we found a solution at orbital period $P$ = 22.10 ± 0.25 days, and with eccentricity $e = 0.19^{+0.30}_{-0.14}$. The mode of the posterior eccentricity distribution is at $e \sim 0.065$, with a long tail towards higher values, and a second peak at $e \sim 0.85$. Because of this, most orbital parameters present a similar bimodal distribution. In particular, the posterior of the RV semi-amplitude $K$ also extends to 277 m s$^{-1}$ (95% confidence level). Using the eccentricity measurement from Nesvorný et al. (2013) as a constraint in our MCMC analysis, we measured an RV amplitude of 48.9 ± 6.0 m s$^{-1}$, which agrees well with their prediction.

The inferred mode of the marginal posterior distributions and their 68.3% confidence intervals are shown in Table 1 for the

[1] $\Delta e/e = 0.01$; $\Delta a/a = 3.8 \times 10^{-4}$; $\Delta i \sim 0.0025°$; $\Delta\omega \sim 0.5°$

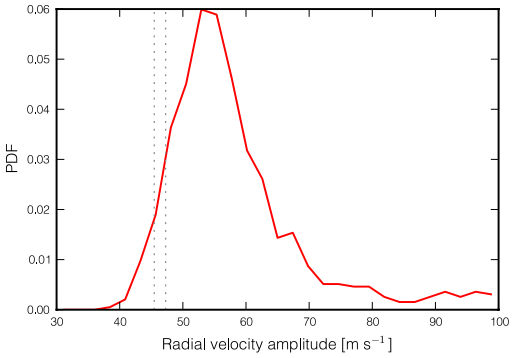


**Fig. 3.** Main peak of the marginalised posterior distribution of the RV semi-amplitude. The dashed vertical lines delimit the 1$\sigma$ range predicted by Nesvorný et al. (2013).

**Table 1.** Parameters for the KOI-142 system at reference epoch $E$ = 2 456 475.40947 BJD$_{\rm UTC}$.

| | |
|---|---|
| Fitted parameters | |
| Orbital period, $P$ [days] | 22.10 ± 0.25 |
| $\sqrt{e}\cos(\omega)$ | −0.32 ± 0.25 |
| $\sqrt{e}\sin(\omega)$ | $0.24^{+0.17}_{-0.29}$ |
| Mean anomaly at epoch [deg] | $298^{+21}_{-77}$ |
| RV amplitude, $K$ [m s$^{-1}$] | $57.4^{+29}_{-7.5}$ |
| Systemic velocity [km s$^{-1}$] | $-20.4547^{+0.0035}_{-0.0085}$ |
| Spectroscopic parameters | |
| Effective temperature [K] | 5460 ± 70 |
| Surface gravity [dex] | 4.6 ± 0.2 |
| Metallicity | 0.25 ± 0.09 |
| Derived parameters | |
| Periapsis passage, $T_{\rm p}$, BJD$_{\rm UTC}$ | 2 456 478.7 ± 2.5 |
| cov($P$, $T_{\rm p}$)$^{\dagger}$ [days$^2$] | –0.00323 |
| Orbital eccentricity | $0.19^{+0.30}_{-0.14}$ |
| Semi-major axis (AU) | 0.1529 ± 0.0021 |
| Minimum planet mass [$M_{\rm J}$] | $0.76^{+0.32}_{0.16}$ |
| $M_{\rm p}\sin i/M_{\rm s} \times 10^4$ | $7.5^{+3.3}_{-1.6}$ |
| Stellar mass, $M_{\rm s}$ [$M_\odot$] | 0.974 ± 0.038 |
| Stellar radius, $R_{\rm s}$ [$R_\odot$] | 0.910 ± 0.040 |
| Age [Gyr] | $3.0^{+3.2}_{-2.0}$ |

**Notes.** $^{(\dagger)}$ Covariance between orbital period and time of periapsis passage.

revised stellar parameters described in Sect. 3. The best-fit model is shown in Fig. 1. In Fig. 3 the marginalised posterior distribution of the RV amplitude is presented. The RV signal agrees well with the prediction by Nesvorný et al. (2013).

A periodogram of the fit residuals does not show any power at the period of the transiting object KOI-142 b. However, it does show a peak at 14.8 days, with an FAP slightly below 10%. Owing to the dynamic evolution of the system, more RVs are necessary to understand the nature of this peak. One possibility is that it is a harmonic of the stellar rotational period. The residuals of the fit, which are consistent with white noise, allow one to derive an upper limit to the mass of the inner planet of 53.9 $M_\oplus$ at the 99% confidence level, which also agrees with the value estimated with TTVs $m_{\rm b}$ = 8.7 ± 2.5 $M_\oplus$ (Nesvorný et al. 2013).

To compute the mass and radius of the stellar host we drew 10 000 samples from the distribution of $T_{\rm eff}$ and [Fe/H] determined in Sect. 3, which was assumed to follow an uncorrelated multi-normal distribution. We combined this with

the stellar density from the transit fit (Nesvorný et al. 2013), corrected for the eccentricity using the posterior samples obtained with the MCMC algorithm. The mass and radius of the star were obtained by interpolation of the Dartmouth stellar tracks (Dotter et al. 2008). Around 70% of the samples fall in an unphysical region of parameter space, where an interpolation is not possible. This is probably because of the correlations between $T_{\rm eff}$, [Fe/H], and the stellar density, which were not taken into account in our procedure. This problem was also encountered by Nesvorný et al. (2013).

With the obtained samples of $M_*$, we computed our posterior distribution for the mass of the planet. These values are reported in Table 1.

## 5. Discussion

We presented radial velocity observations of KOI-142 with the SOPHIE spectrograph at the Observatoire de Haute-Provence. These measurements allowed us to confirm the discovery of a non-transiting planet in the KOI-142 system, KOI-142c, which agrees with the TTV predictions of Nesvorný et al. (2013) and provides an independent validation of the TTV method. The estimated RV semi-amplitude of KOI-142b, $K_{\rm b} = 2.6\,{\rm m\ s^{-1}}$ (Nesvorný et al. 2013), is below the current sensitivity of our RV measurements, and hence the known transiting planet is not included in our analysis. We preformed an MCMC analysis of the RVs using a Keplerian model with non-informative priors in all the parameters. We estimated the orbital period of planet c, $P_{\rm c} = 22.10 \pm 0.25$ days and the RV semi-amplitude, $K_{\rm c} = 57.4^{+29}_{-7.5}$ m s$^{-1}$. In this way we confirmed the parameters of KOI-142c predicted by the dynamic analysis of transit variations by Nesvorný et al. (2013), using RV observations. According to the dynamic TTV analysis, KOI-142c is observed close to edge-on ($\iota = 3.8 \pm 1.6°$) and hence the planet true mass is expected to be close to the our estimated minimum mass of $0.76^{+0.32}_{0.16}\,M_{\rm Jup}$.

The confirmation of a TTV prediction is important not just to validate the method, but also because unknown (non-transiting) companions might affect the observed TTVs and add further uncertainty to the already complex TTV inversion problem. Another *Kepler* planetary system, KOI-94 (Borucki et al. 2011), is one of the few TTV systems for which it was possible to constrain the mass of three transiting planets, KOI-94c, KOI-94d, and KOI-94e by RV observations and subsequently by TTVs (no TDVs were measured in KOI-94). However, for the more massive planet, KOI-94d, a large discrepancy between the mass derived from RV measurements and the mass derived from TTVs was found. The RV derived mass, $m_{\rm d} = 106 \pm 11\ M_\oplus$ (Weiss et al. 2013), is approximately twice the mass predicted from TTVs, $m_{\rm d} = 52^{+0.9}_{-7.1}\ M_\oplus$ according to Masuda et al. (2013). These authors suggested the presence of other planets in the system as a possible cause of the discrepancy. The good agreement found for KOI-142 between the TTV prediction and the RV observations presented here implies that the TTVs of KOI-142b are unaffected by other possible planets in the system. A combined RV and TTV analysis of this system will allow one to set limits on the presence of other companions and better characterise the planets. This is beyond the scope of this paper.

The configuration of multi-planetary systems gives insight into their formation and dynamical evolution (Kley & Nelson 2012). Like many *Kepler* candidates (Lissauer et al. 2011b; Fabrycky et al. 2012), the KOI-142 planet pair is just wide of the 2:1 resonance. As mentioned by Nesvorný et al. (2013), the eccentricity of KOI-142c derived from the dynamic analysis of TTVs and TDVs, $e_{\rm c} = 0.05628 \pm 0.0021$, is higher than expected from the gravitational interaction of the two planets (Lee et al. 2013). Moreover, tidal damping can only explain this system if the dissipation efficiency of the inner planet was ~6.5 higher than expected for a planet of this type (Lee et al. 2013). However, since planet c is capable of opening a gap on the disc, planet-disc interaction (Baruteau & Papaloizou 2013) or planet-planet interaction within the disc (Lega et al. 2013) might be able to explain the current configuration. More RV observations together with a dynamic analysis of the system will bring valuable insight into the formation history of this remarkable system.

*Acknowledgements.* We thank the staff at Haute-Provence Observatory. We acknowledge the PNP of CNRS/INSU, and the French ANR for their support. The team at LAM acknowledges support by grants 98761 (SCCB), 251091 (JMA) and 426808 (CD). R.F.D. was supported by CNES via its postdoctoral fellowship program. A.S. acknowledges the support of the European Research Council/European Community under the FP7 through Starting Grant agreement number 239953. A.S.B. gratefully acknowledges support through INAF/HARPS-N fellowship.

## References

Agol, E., Steffen, J., Sari, R., & Clarkson, W. 2005, MNRAS, 359, 567
Ballard, S., Fabrycky, D., Fressin, F., et al. 2011, ApJ, 743, 200
Baranne, A., Queloz, D., Mayor, M., et al. 1996, A&AS, 119, 373
Barros, S. C. C., Boué, G., Gibson, N. P., et al. 2013, MNRAS, 430, 3032
Baruteau, C., & Papaloizou, J. C. B. 2013, ApJ, 778, 7
Bonomo, A. S., Santerne, A., Alonso, R., et al. 2010, A&A, 520, A65
Borucki, W. J., Koch, D. G., Basri, G., et al. 2011, ApJ, 728, 117
Bouchy, F., Hébrard, G., Udry, S., et al. 2009, A&A, 505, 853
Bouchy, F., Bonomo, A. S., Santerne, A., et al. 2011, A&A, 533, A83
Boué, G., Oshagh, M., Montalto, M., & Santos, N. C. 2012, MNRAS, 422, L57
Bruntt, H., Bedding, T. R., Quirion, P.-O., et al. 2010a, MNRAS, 405, 1907
Bruntt, H., Deleuil, M., Fridlund, M., et al. 2010b, A&A, 519, A51
Chambers, J. E. 1999, MNRAS, 304, 793
Díaz, R. F., Almenara, J. M., Santerne, A., et al. 2013, MNRAS, submitted
Dotter, A., Chaboyer, B., Jevremović, D., et al. 2008, ApJS, 178, 89
Fabrycky, D. C., Lissauer, J. J., Ragozzine, D., et al. 2012, ApJ, submitted [arXiv:1202.6328]
Ford, E. B., Rowe, J. F., Fabrycky, D. C., et al. 2011, ApJS, 197, 2
Gibson, N. P., Pollacco, D., Simpson, E. K., et al. 2009, ApJ, 700, 1078
Holman, M. J., & Murray, N. W. 2005, Science, 307, 1288
Holman, M. J., Fabrycky, D. C., Ragozzine, D., et al. 2010, Science, 330, 51
Kley, W., & Nelson, R. P. 2012, ARA&A, 50, 211
Lee, M. H., Fabrycky, D., & Lin, D. N. C. 2013, ApJ, 774, 52
Lega, E., Morbidelli, A., & Nesvorný, D. 2013, MNRAS, 431, 3494
Lissauer, J. J., Fabrycky, D. C., Ford, E. B., et al. 2011a, Nature, 470, 53
Lissauer, J. J., Ragozzine, D., Fabrycky, D. C., et al. 2011b, ApJS, 197, 8
Masuda, K., Hirano, T., Taruya, A., Nagasawa, M., & Suto, Y. 2013, ApJ, 778, 185
Mazeh, T., Nachmani, G., Holczer, T., et al. 2013, ApJS, 208, 16
Meschiari, S., & Laughlin, G. P. 2010, ApJ, 718, 543
Miller-Ricci, E., Rowe, J. F., Sasselov, D., et al. 2008, ApJ, 682, 593
Miralda-Escudé, J. 2002, ApJ, 564, 1019
Nesvorný, D., & Morbidelli, A. 2008, ApJ, 688, 636
Nesvorný, D., Kipping, D. M., Buchhave, L. A., et al. 2012, Science, 336, 1133
Nesvorný, D., Kipping, D., Terrell, D., et al. 2013, ApJ, 777, 3
Pepe, F., Mayor, M., Galland, F., et al. 2002, A&A, 388, 632
Perruchot, S., Kohler, D., Bouchy, F., et al. 2008, in SPIE Conf. Ser., 7014
Santerne, A., Díaz, R. F., Moutou, C., et al. 2012, A&A, 545, A76
Steffen, J. H., Fabrycky, D. C., Ford, E. B., et al. 2012a, MNRAS, 421, 2342
Steffen, J. H., Ford, E. B., Rowe, J. F., et al. 2012b, ApJ, 756, 186
Veras, D., Ford, E. B., & Payne, M. J. 2011, ApJ, 727, 74
Weiss, L. M., Marcy, G. W., Rowe, J. F., et al. 2013, ApJ, 768, 14
Zechmeister, M., & Kürster, M. 2009, A&A, 496, 577

**Table 2.** Radial velocity measurements for KOI-142.

| $BJD_{UTC}$ –2 456 000 | RV (km s$^{-1}$) | $\sigma_{RV}$ (km s$^{-1}$) | Bis (km s$^{-1}$) | $T_{exp}$ (s) | $S/N$/pix (550 nm) |
|---|---|---|---|---|---|
| 475.40947 | –20.423 | 0.010 | –0.072 | 1800 | 25.9 |
| 481.50789 | –20.521 | 0.016 | –0.040 | 1803 | 17.3 |
| 505.56661 | –20.491 | 0.012 | –0.051 | 815 | 17.7 |
| 508.60654 | –20.470 | 0.013 | –0.061 | 1800 | 16.6 |
| 514.56435 | –20.400 | 0.015 | –0.034 | 3600 | 18.8 |
| 533.36529 | –20.409 | 0.009 | –0.073 | 1800 | 25.5 |
| 537.45558 | –20.408 | 0.008 | –0.038 | 3600 | 24.8 |
| 551.44399* | –20.473 | 0.011 | –0.101 | 3600 | 21.9 |
| 582.35976* | –20.414 | 0.010 | –0.050 | 3600 | 27.0 |
| 597.30019 | –20.465 | 0.008 | –0.024 | 3600 | 33.4 |
| 611.24418* | –20.499 | 0.013 | –0.015 | 3600 | 19.8 |

**Notes.** Asterisks show the measurements corrected for background light.

**Table 3.** Relative abundances of the main elements of KOI-142.

| Element | Abundance (dex) |
|---|---|
| Si I | 0.33 ± 0.15 |
| Sc II | 0.39 ± 0.15 |
| Ti I | 0.22 ± 0.15 |
| Ti II | 0.30 ± 0.19 |
| V I | 0.41 ± 0.15 |
| Co I | 0.36 ± 0.15 |
| Cr I | 0.27 ± 0.15 |
| Cr II | 0.16 ± 0.15 |
| Fe I | 0.25 ± 0.15 |
| Fe II | 0.25 ± 0.16 |
| Ni I | 0.29 ± 0.15 |
| Y II | –0.04 ± 2.01 |